X-ray Polarization Measurements at Relativistic Laser Intensities

P. Beiersdorfer[1], R. Shepherd[1], R. C. Mancini[2], H. Chen[1], J. Dunn[1], R. Keenan[1], J. Kuba[1], P. K. Patel[1]
Y. Ping[1], D. F. Price[1], K. Widmann[1]
[1] *Lawrence Livermore National Laboratory, Livermore, CA 94550, USA*
[2] *University of Nevada, Reno, NV 89557, USA*

An effort has been started to measure the short pulse laser absorption and energy partition at relativistic laser intensities up to 10^{21} W/cm^2. Plasma polarization spectroscopy is expected to play an important role in determining fast electron generation and measuring the electron distribution function.

I. INTRODUCTION

Plasma polarization spectroscopy (PPS) has been employed to verify and study the existence of non-thermal, fast electrons in laser-plasma interaction since the first experiments by Kieffer *et al.* [1–3]. The laser intensity in these measurements has been in the range $10^{14} - 10^{16}$ W/cm^2. Measurements of laser absorption at higher intensities $\leq 10^{18}$ W/cm^2 have been made [4] but without employing x-ray polarimetry. Theoretical studies of fast-electron generation and their effect on the x-ray linear polarization have been made [5,6], which considered laser intensities as high as 10^{18} W/cm^2.

Here we describe a planned effort to use PPS as a diagnostic for determining fast electron generation and energy partition of short pulse lasers interacting with matter at relativistic laser intensities up to 10^{21} W/cm^2.

II. PHYSICS LASERS AT LLNL

The Physics and Advanced Technologies Directorate at the University of California Lawrence Livermore National Laboratory operates four powerful multi-purpose laser facilities used for experiments in high-energy density physics, x-ray laser development, and material science. These facilities are used in collaborative experiments with many non-LLNL user, and new collaborations are always welcome. In fact, the planned PPS experiment respresents a collaboration between LLNL and the University of Nevada in Reno.

The first of these lasers is the Compact Multipulse Terawatt (COMET) laser operating at 1.054 μm. A schematic of the facility is shown in Fig. 1. The laser consists of a Ti:sapphire oscillator with glass amplifiers that can generate and probe plasmas with up to four beams. One or two long pulse beams (Δt = 600 ps) with 15 and 4 J, respectively, are available together with two or three short pulse beams (Δt = 500 fs) with 1 or 7.5 J. One of the short pulse beams is equipped for operation frequency doubled or tripled laser light. A summary of the parameters of the COMET laser is given in Table I.

The COMET laser has been used mainly for developing efficient x-ray laser schemes [7,8]. The multi-pulse capability has been used to generate an additional plasma on a slab that in turn is probed with the x-ray laser pulse generated by the other COMET laser beams [9].

TABLE I. Parameters of the COMET laser.

Beam type	Energy (J)	Pulse Length (ps)
Long pulse	15	600
Short pulse	7.5	0.5
Beam 3	1	0.5
Beam 3	4	600
Probe beam		0.5[a]

[a] At 2ω or 3ω emission, i.e., 527 nm and 351 nm, respectively.

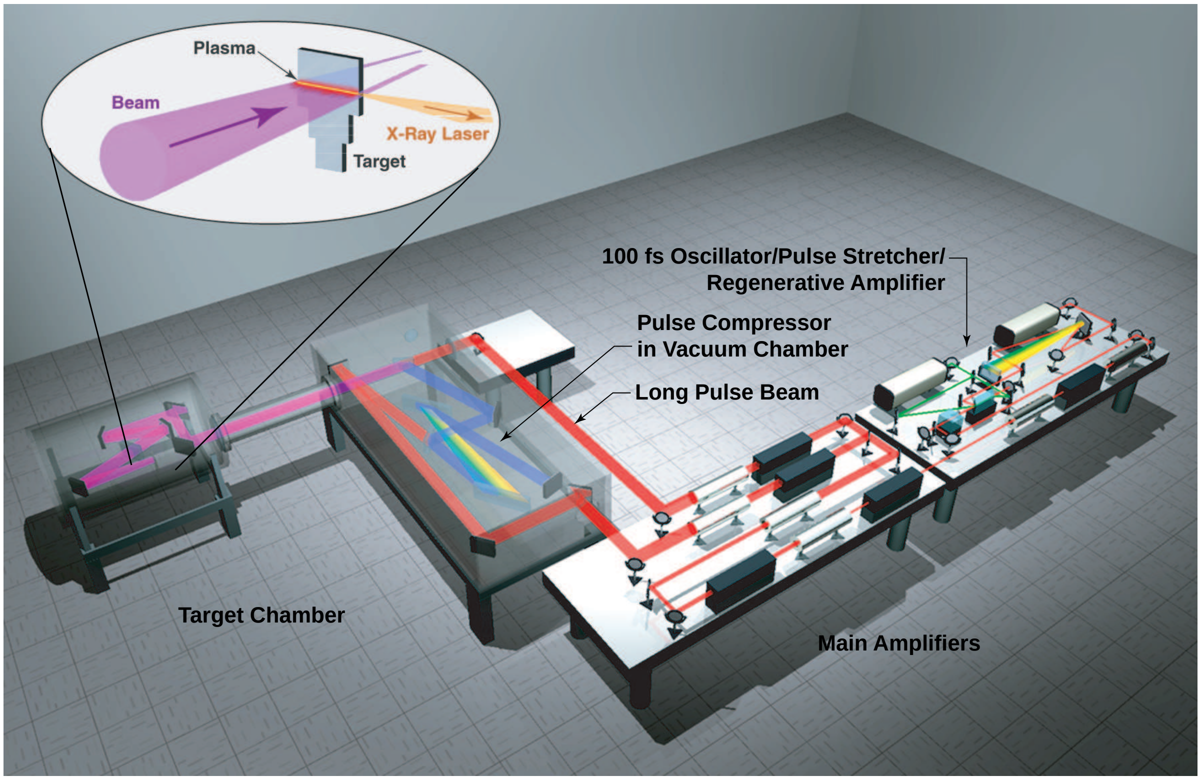

FIG. 1. Schematic of the COMET laser.

The second of the physics lasers is the Ultra Short Pulse (USP) laser, shown schematically in Fig. 2. USP is a Ti:Sapphire laser operating either at 800 nm with an energy of 1 J or at 400 nm with an energy of 0.35 J. The pulse width of the USP laser is ≥ 80 fs; the spot size is less than three times the diffraction limit, i.e., about 1–2 μm at 400 nm (about 3 μm at 800 nm). As a result, USP has an intensity as high as 5×10^{19} W/cm^2. The contrast between prepulse and main pulse is 10^5 at 1ω and 10^7 at 2ω. Short pulse laser energy of 100–120 mJ is available at 10 Hz repetition rate and at about 20/hour at higher energies. A summary of the parameters of the USP laser is given in Table II.

TABLE II. Parameters of the USP laser.

Wavelength (nm)	Energy (J)	Pulse Length (fs)	Spot Size μm
800	1	≥ 80	3
400	0.35	≥ 80	1–2

Currewntly, the USP laser is being used for atomic physics studies of hot, high-density plasma [10] and equation of state related conductivity studies of warm-dense matter [11,12].

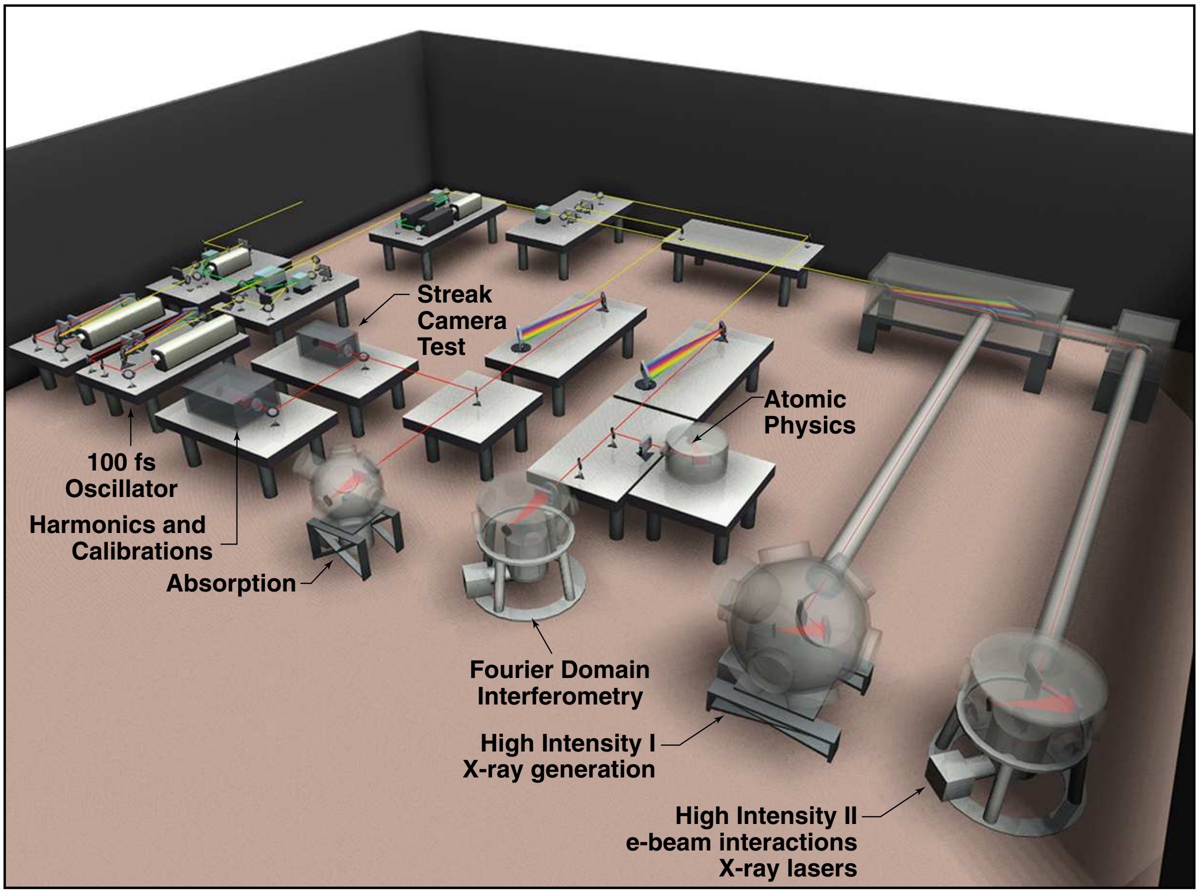

FIG. 2. Schematic of the USP laser.

The third laser is the Janus laser, which is shown schematically in Fig. 3. This facility has been operating since the early 1970s when it was commissioned for studies of inertial confinement fusion (ICF). Janus is a two-beam laser (hence its name), providing 300 J per beam on target. When the primary ICF studies on Janus were replaced with studies on the Argus laser and later on the Shiva and Nova lasers, the emphasis of the Janus facility was shifted to ICF support studies and ICF diagnostics development. It has also been used for x-ray laser studies [13]. Like these subsequent lasers, Janus can operate at 1064 nm as well as the double and triple frequency, as summarized in Table III. The pulse width can be varied from 100 ps to greater than 6 ns. Beam smoothing was added in 1999. The spot size is 17 μm, and up to three shots per hour can be accomodated. An upgrade to 1000 J per beam is currently under way.

TABLE III. Parameters of the Janus laser.

Parameter	Value
Wavelength	1064 nm, 532 nm, 366 nm
Energy	300 J at 1064 nm
Pulse width	0.1 – 6 ns
Spot size	17 μm
Repetition rate at rod shot energies (2–20 J)	20 shots per hour
Repetition rate at maximum energy	2 per hour

An important feature is that one of the Janus beams (at 532 nm) can be used to pump a second ultra short pulse laser. The ultra short pulse laser pumped by Janus has been dubbed JanUSP [14]. A schematic of JanUSP is shown in Fig. 4.

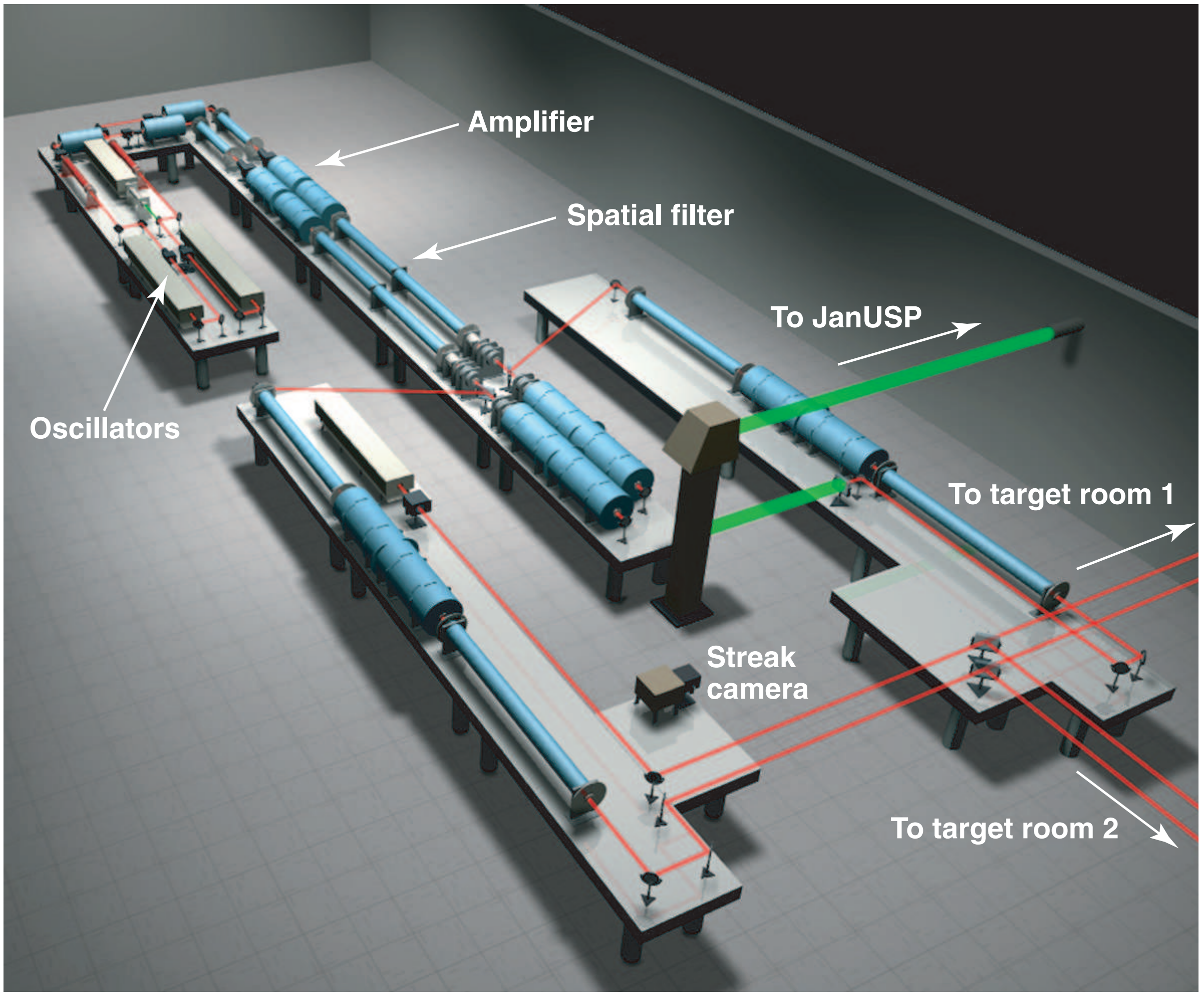

FIG. 3. Schematic of the Janus laser.

TABLE IV. Parameters of the Janus-pumped ultra short pulse laser JanUSP.

Parameter	Value
Wavelength	800 nm
Energy	15 J
Pulse width	$\geq$ 80 fs
Spot size	$\leq$ 3 μm
Repetition rate in low-power mode (300 mJ)	10 Hz
Repetition rate at maximum energy	2 per hour

Like USP, JanUSP is a Ti:Sapphire laser. But being pumped by Janus it can reach energies of 15 J at 800 nm and high peak power in excess of 150 TW. The focussing spot of JanUSP is two times the diffraction limit ($\leq 3\mu$m), which is better than that of the USP laser; the pulse width is about the same at ≥ 80 fs. As a result of these operating parameters the JanUSP laser can focus up to 10^{21} W/cm^2 on target. The contrast between the prepulse and the main pulse is in the range of 10^9 and may be improved by implementing a frequency doubling crystal. The repetition rate is 2 shots per hour. Parameters of the JanUSP laser are given in Table IV.

JanUSP can also be operated in a low-energy mode with 300 mJ per shot at a repetition rate of 10 Hz. This capability is currently being used to develop high repetition rate x-ray laser schemes [15].

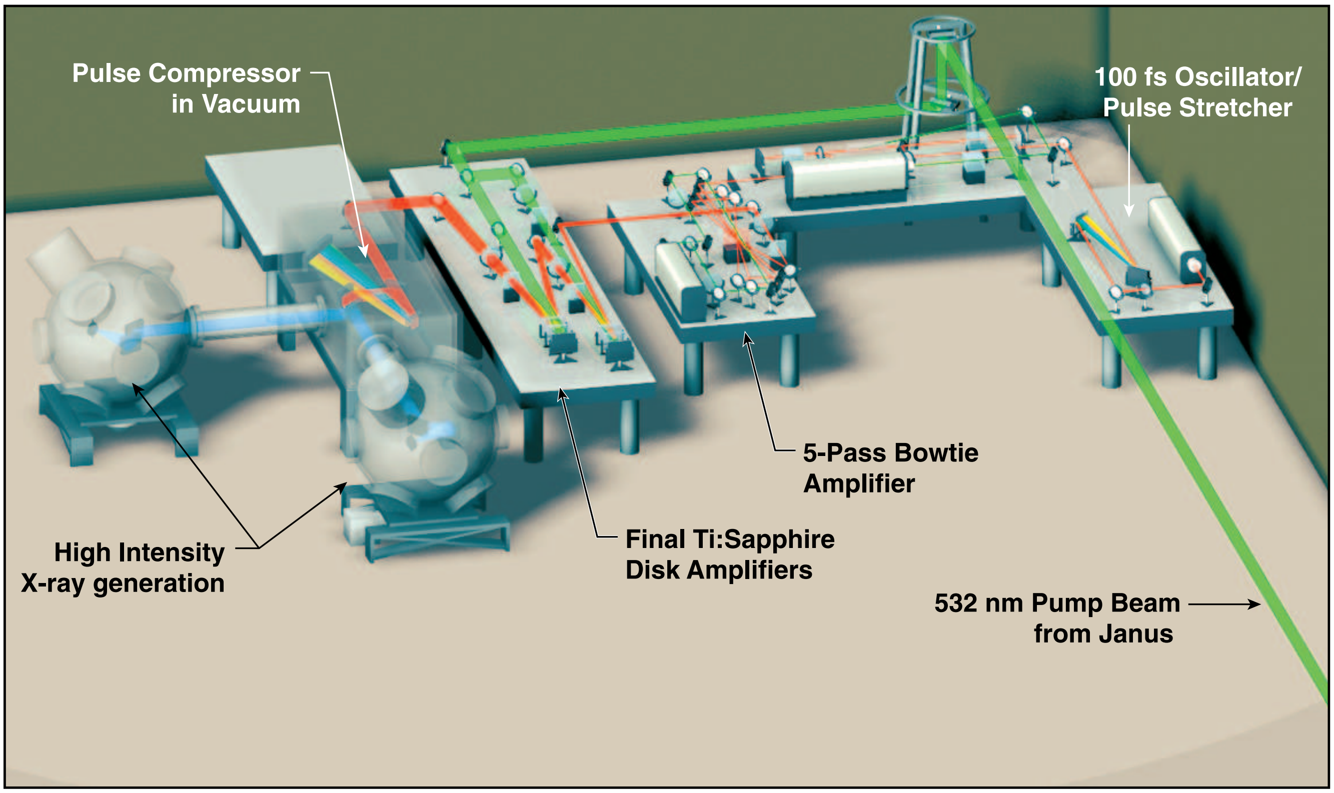

FIG. 4. Schematic of the JanUSP laser.

JanUSP has been used for beam generation experiments. In particular, it has been used for energy partition and γ-ray beam generation experiments [16,17]. About one to two percent of the laser energy can be converted into a proton beam emanating from the back surface of a thin (10–20 μm) aluminum foil propagating at energies up to 20–25 MeV [16]. Detection of the proton beam was by radiochromatic film.

Electron beam generation from the back (and front) side of foil targets has also been observed [18]. For this an electron spectrometer was built utilizing permanent magnets for energy analysis and a charge couple device camera for read out that can measure electrons with energies between 100 keV and 60 MeV [18]. It is possible that up to half of the total laser energy is converted to fast electrons at the high intensities possible with JanUSP.

III. PLANNED EXPERIMENTS

Laser absorption at intensities close to 10^{18} W/cm^2 was studied by Price et al. employing the USP laser [4]. They showed that absorption by inverse bremsstrahlung is replaced by relativistic $J \times B$ heating at a laser intensity near 10^{17} W/cm^2. As the intensity is increased further additional absorption mechanisms may play an important role such as ion shock formation and vacuum (Brunel) heating. Moreover, there is a relativistic increase in the electron's mass making the electron response to the oscillating laser field more sluggish and thus allowing the laser to penetrate deeper by increasing the critical density. The pondermotive pressure will steepen the density profile above the target surface and thus will affect the electron and ion transport. Also, ultra-high electric and magnetic fields can be generated that change the absorption at very high intensities. The magnetic field may reach values as high as 3 gigagauss; the electric field may reach values of 10^{12} V/cm. The interplay of all of these processes has not been systematically studied at high laser intensities, but it needs to be known as petawatt lasers are being put in use for physics studies.

We are planning to study laser absorption in a sytematic and controlled way, and PPS will play an important role. X-ray emission measurements are planned to determine the relative fraction of the hot electron component relative to the thermal component. These will involve studies of K-alpha generation by fast electrons as a function of plasma density. The experimental scheme to perform such experiments is shown in Fig. 5.

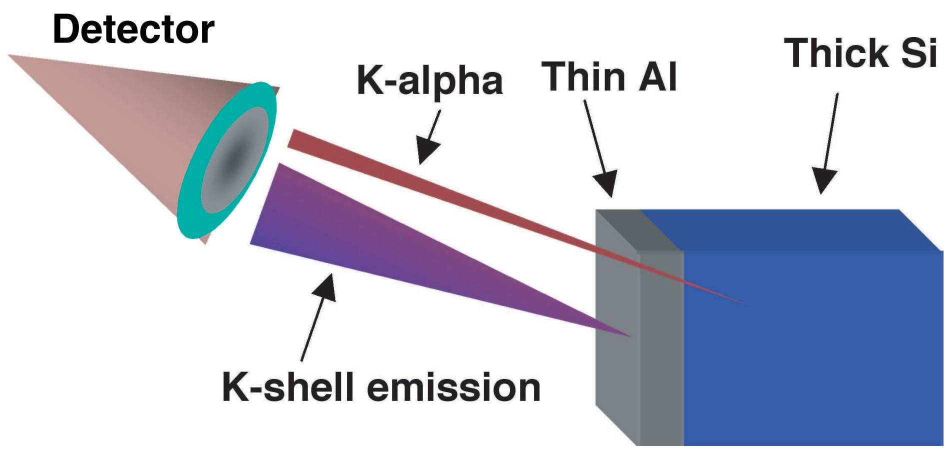

FIG. 5. Schematic of the setup to measure the K-alpha emission of silicon produced by fast electrons from the laser-heated aluminum target.

Moreover, time-dependent measurements of the x-ray emission are planned that are sensitive to the collisional dynamics of thermal and hot electrons, as shown schematically in Fig. 6. For such measurements fast streak cameras are needed. We have developed x-ray cameras with 500 fs time resolution [19]. These measurements will also resolve the polarization of the x-ray lines by operating our cylindrically bent crystal spectrometers near the Brewster angle.

IV. ACKNOWLEDGEMENT

This work was performed under the auspices of the U.S. DOE by the University of California Lawrence Livermore National Laboratory under contract W-7405-Eng-48.

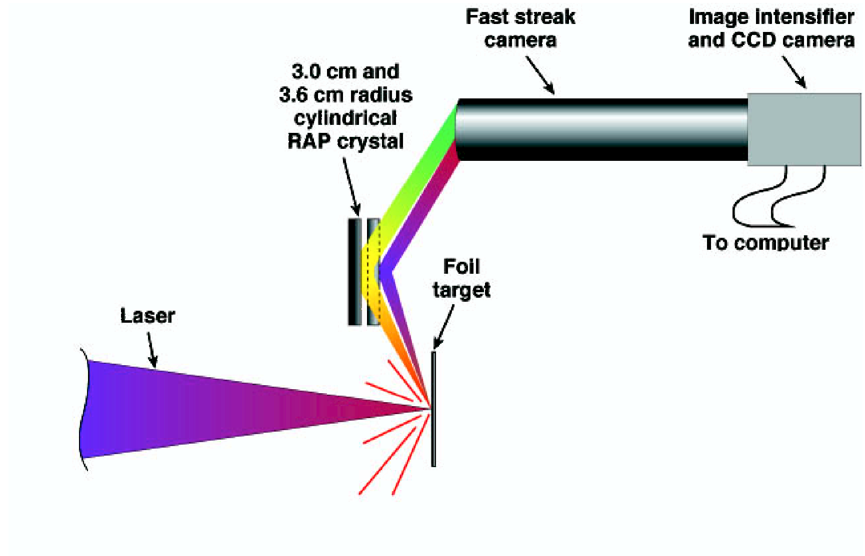

FIG. 6. Schematic of the setup to measure the x-ray spectra using high-resolution von Hámos-type crystal spectrometers and fast streak cameras.

[1] J. C. Kieffer, J. P. Matte, H. Pépin, M. Chaker, Y. Beaudoin, T. W. Johnston, C. Y. Chien, S. Coe, G. Mourou, and J. Dubau, Phys. Rev. Lett. **68**, 480 (1992).

[2] J. C. Kieffer, J. P. Matte, M. Chaker, Y. Beaudoin, C. Y. Chien, S. Coe, G. Mourou, J. Dubau, and M. K. Inal, Phys. Rev. E **48**, 4648 (1993).

[3] H. Yoneda, N. Hasegawa, S. ichi Kawana, and K. ichi Ueda, Phys. Rev. E **56**, 988 (1997).

[4] D. F. Price, R. M. Moore, R. S. Walling, G. Guethlein, R. L. Shepherd, R. E. Stewart, and W. E. White, Phys. Rev. Lett. **75**, 252 (1995).

[5] P. Hakel, R. C. Mancini, J.-C. Gauthier, E. Mínguez, J. Dubau, and M. Cornille, Rev. Sci. Instrum. **72**, 1245 (2001).

[6] P. Hakel, R. C. Mancini, J.-C. Gauthier, E. Mínguez, J. Dubau, and M. Cornille, Phys. Rev. E in press, .

[7] J. Dunn, R. F. Smith, J. Nilsen, H. Fiedorowicz, A. Bartnik, and V. N. Shlyaptsev, J. Opt. Soc. Am. B **20**, 203 (2003).

[8] R. F. Smith, J. Dunn, J. R. Hunter, J. Nilsen, S. Hubert, S. Jacquemot, C. Remond, R. Marmoret, M. Fajardo, P. Zeitoun, L. Vanbostal, C. L. S. Lewis, M. F. Ravet, and F. Delmotte, Opt. Lett. **28**, 2261 (2003).

[9] R. F. Smith, J. Dunn, J. Nilsen, V. N. Shlyaptsev, S. Moon, J. Filevich, J. J. Rocca, M. C. Marconi, J. R. Hunter, and T. W. Barbee, Phys. Rev. Lett. **89**, 065004 (2002).

[10] P. Audebert, R. shepherd, K. B. Fournier, O. Peyrusse, D. Price, R. Lee, P. Springer, J.-C. Gauthier, and L. Klein, Phys. Rev. Lett. **89**, 265001 (2002).

[11] K. Widmann, G. Guethlein, M. E. Foord, R. C. Cauble, F. G. Patterson, D. F. Price, F. J. Rogers, P. T. Springer, R. E. Stewart, A. Ng, T. Ao, and A. Forsman, Phys. Plasmas **8**, 3869 (2001).

[12] K. Widmann, T. Ao, M. E. Foord, D. F. Price, A. D. Ellis, P. T. Springer, and A. Ng, Phys. Rev. Lett. in press, .

[13] J. Dunn, A. L. Osterheld, R. Shepherd, W. E. White, V. N. Shlyaptsev, and R. E. Stewart, Phys. Rev. Lett. **80**, 2825 (1998).

[14] J. D. Bonlie, F. Patterson, D. Price, B. White, and P. Springer, Appl. Phys. B **70**, S155 (2000).

[15] R. Keenan, J. Dunn, V. N. Shlyaptsev, R. F. Smith, P. K. Patel, and D. F. Price, Proc. SPIE Int. Soc. Opt. Eng. **5197**, 213 (2003).

[16] P. K. Patel, A. J. Mackinnon, M. H. Key, T. E. Cowan, M. E. Foord, M. Allen, D. F. Price, H. Ruhl, P. T. Springer, and R. Stephens, Phys. Rev. Lett. **91**, 125004 (2003).

[17] M. Allen, P. K. Patel, A. Mackinnon, D. F. Price, S. Wilks, and E. Morse, Phys. Rev. Lett. submitted, .

[18] H. Chen, P. K. Patel, D. F. Price, B. K. Young, P. T. Springer, R. Berry, R. Booth, C. Bruns, and D. Nelson, Rev. Sci. Instrum. **74**, 1551 (2003).

[19] J. Kuba, R. Shepherd, R. Booth, R. E. Stewart, E. C. W. Lee, P. Audebert, J. K. Crane, R. R. Cross, J. Dunn, and P. T. Springer, Proc. SPIE Int. Soc. Opt. Eng. **5194**, 183 (2004).